




## Research Article

# Study of SiC/graphite particulates on the corrosion behavior of Al 6065 MMCs using tafel polarization and impedance

N. Sunitha<sup>1</sup>  · K. G. Manjunatha<sup>2</sup> · Saifulla Khan<sup>2</sup> · M. Sravanthi<sup>2</sup>

© Springer Nature Switzerland AG 2019

## Abstract

Aluminum metal matrix composites (MMC) have better mechanical properties than the alloy because of high strength-to-density ratios. In addition these composites exhibit low co-efficient of thermal expansion, high corrosion resistance. Al 6065 is the base metal selected for corrosion studies. Al 6065 MMCs are prepared by stir casting method. MMCs are prepared with reinforcement of particulates such as SiC and graphite. Composites are prepared by adding 2, 4 wt % of SiC particulates and hybrid composite with equal amount of SiC and graphite. Base metal alloy without adding any reinforcement is also casted in the same manner for comparison. Present research work involves the study of corrosion behavior of Al 6065 MMCs and the base metal alloy in different mediums using tafel polarization technique and Impedance. The corrosion medium used is 0.1 M acid chloride, 0.1 M acid sulphate and neutral chloride solution of 3.5%. The study is also compiled by SEM analysis of the corroded samples which depicts the deteriorated surfaces. Results indicate that Al 6065 hybrid composite is resistant towards corrosion because of its low percentage of graphite.

**Keywords** Al 6065 · Tafel polarization · Impedance · EIS · SEM

## 1 Introduction

The term “composite” broadly refers to a material system which is comprised of reinforcement distributed in matrix and which procure its distinguishing characteristics from the properties of its reinforcement, geometry and construction of the constituents and from the properties of the interfaces between different constituents [1]. Properties of MMCs strongly depend on the interfacial phenomena between the metal matrix and ceramic reinforcement [2–5]. The main cause of the corrosion in MMCs are reported as (a) galvanic coupling between the matrix and the reinforcement materials (b) formation of an interfacial phase between the reinforcement and matrix (c) micro structural changes processing contaminants resulted from manufacture of the MMC [6, 7]. Addition of low graphite percentages into pure aluminum was found to increase

the corrosion of aluminum in 3.5% NaCl solution due to the activation effect for graphite towards the corrosion of aluminum [8, 9]. Chemical degradation of reinforcements and intermetallic phases cannot be detected by polarization techniques [10].

## 2 Experimental

### 2.1 Materials preparation

Al 6065 is selected as matrix material. Chemical composition of Al 6065 matrix material is given in the Table 1.

Aluminum ingots with 96.11 wt % commercial purity is used as matrix material which is procured from Fensee Metallurgical. Reinforcement material used is micron sized SiC particles and graphite particulates. The method

✉ N. Sunitha, suninair\_hello@yahoo.co.in; K. G. Manjunatha, gopimanju1984@gmail.com; Saifulla Khan, saifullakhan19j@gmail.com; M. Sravanthi, sravanthimagunta@gmail.com | <sup>1</sup>Department of Chemistry, City Engineering College, Kanakapura Road, Bangalore 560062, India. <sup>2</sup>Department of Chemistry, Ghousia College of Engineering, Ramanagaram 562159, India.



**Table 1** Composition of Al6065 alloy (Wt %)

Element	Cu	Fe	Mg	Si	Zn	Ti	Bi	Zr	Cr	Mn	Al
% Composition	0.274	0.4	1.028	0.609	0.06	0.06	1.25	0.12	0.03	0.05	96.11

adopted is stir casting technique. Ingots are melted using electrical resistance furnace [11]. Matrix melt is stirred rigorously at a speed of 450 rpm and a vortex is created at the surface of the melt. Pre-heated, uncoated SiC particulates are introduced into the vortex. Composites containing 2, 4 wt % of SiC particulates and hybrid composite with equal amount of SiC and graphite are casted. In the same manner Al 6065 base metal alloy without any particulates is also casted for comparison. Molten melt is poured into steel moulds. Casted materials were cut into rectangular test coupons of length 6 cm, width 2.25 cm and thickness 4.95 mm using abrasive cutting wheel. Dimensions were measured using Vernier gauge. Rectangular specimens were grounded using different SiC grade emery papers like 80,100, 200,400 and 800. Before mounting for the electrochemical analysis the specimens were polished on polishing wheel using diamond paste to obtain a mirror finish by following standard metallographic techniques. Finally degreased in acetone and dried. Stock solutions of 0.1 M HCl and 0.1 M H<sub>2</sub>SO<sub>4</sub> of analytical grade are prepared using distilled water. Similarly analytical grade NaCl solution of 3.5% concentration is also prepared using distilled water.

## 2.2 Electrochemical testing method

Electrochemical measurements are carried out using electrochemical work station of model 608 E-series procured from CH Instruments, USA having software version 12.04. Three electrode compartment cell made up of Pyrex glass with Ag/AgCl electrode (1 M KCl is filled) as reference electrode, platinum electrode as auxiliary electrode and rectangular Al 6065 specimen of 6 cm length, 2.25 cm width and 4.95 mm thickness used as working electrode for electrochemical measurements. Electrodes were placed in their respective positions in the electrochemical cell as shown in Fig. 1. This process is carried out at room temperature.

### 2.2.1 Tafel polarization

Polarization technique were used to obtain the micro cell corrosion rates [12]. Mirror finished surfaces of Al 6065 rectangular composites and the base metal alloy were allowed to come in contact with different concentrations of electrolytes like 0.1 M HCl, 0.1 M H<sub>2</sub>SO<sub>4</sub> and 3.5% NaCl at room temperature. Specimens were in contact with

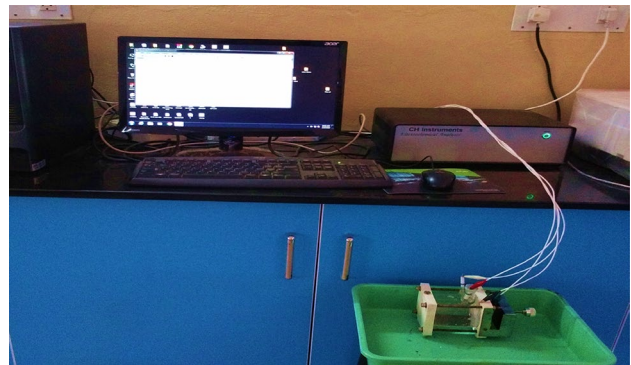


**Fig. 1** Electrochemical work station of model 608 E-series

the respective electrolyte solutions for 400 s to get steady open circuit potential (OCP). Polarization curves were recorded by polarizing the specimen to  $-250$  mV cathodically and  $+250$  mV anodically with respect to OCP at a scan rate of 1 mV/s.

### 2.2.2 Electrochemical impedance spectroscopy

Complex plane plots were obtained over a frequency range from  $10^{-5}$  Hz to 1 MHz using an amplitude AC signal of 5 mV. At room temperature first open circuit potential of the working electrode is measured using different corrodents, later impedance measurements were carried out.

## 2.3 Scanning electron microscopy (SEM) analysis

Rectangular specimens of Al 6065 are grounded using SiC grade emery paper of grit size ranging from 80 to 800 as mentioned earlier and mirror finished. Specimens were subjected to electrochemical testing method and SEM micrographs were analyzed.

## 3 Results

### 3.1 Micro characteristics analysis

Micrographs depicts that in hybrid composite and in Al 6065 base metal alloy surfaces were less deteriorated by the corrodents. As SiC is a semiconductor disintegration of matrix occurs at Al/SiC interface in the

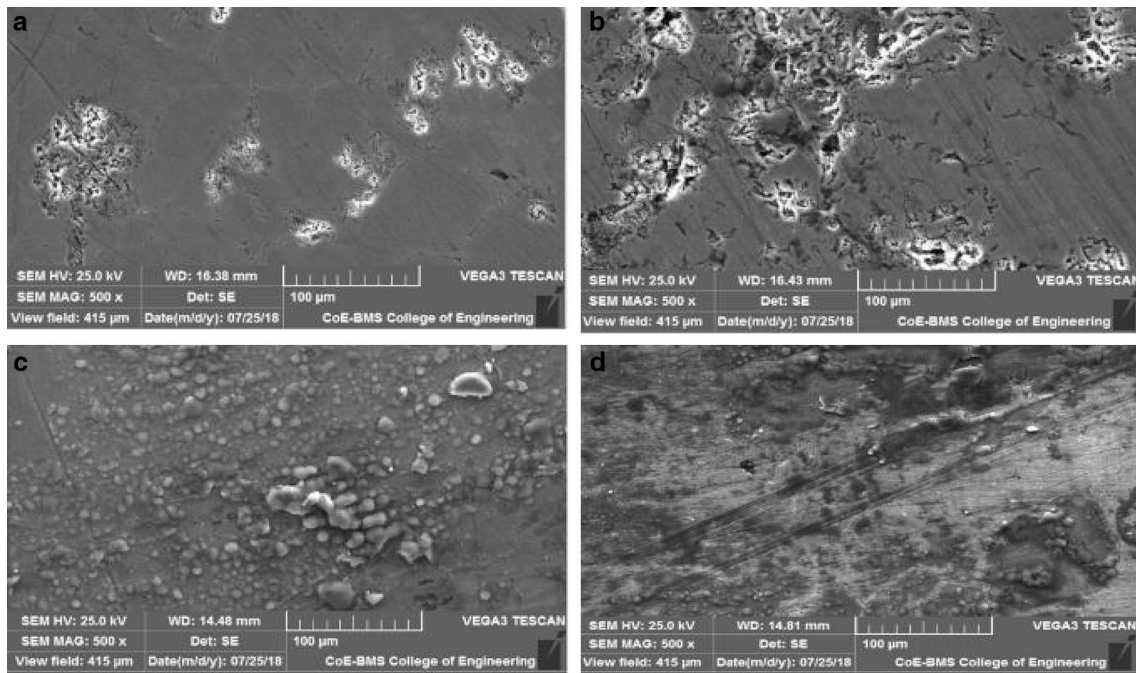


**Fig. 2** SEM micrographs of polarized samples of Al 6065 base metal alloy, 2%, 4% and hybrid composites in 0.1 M HCl medium

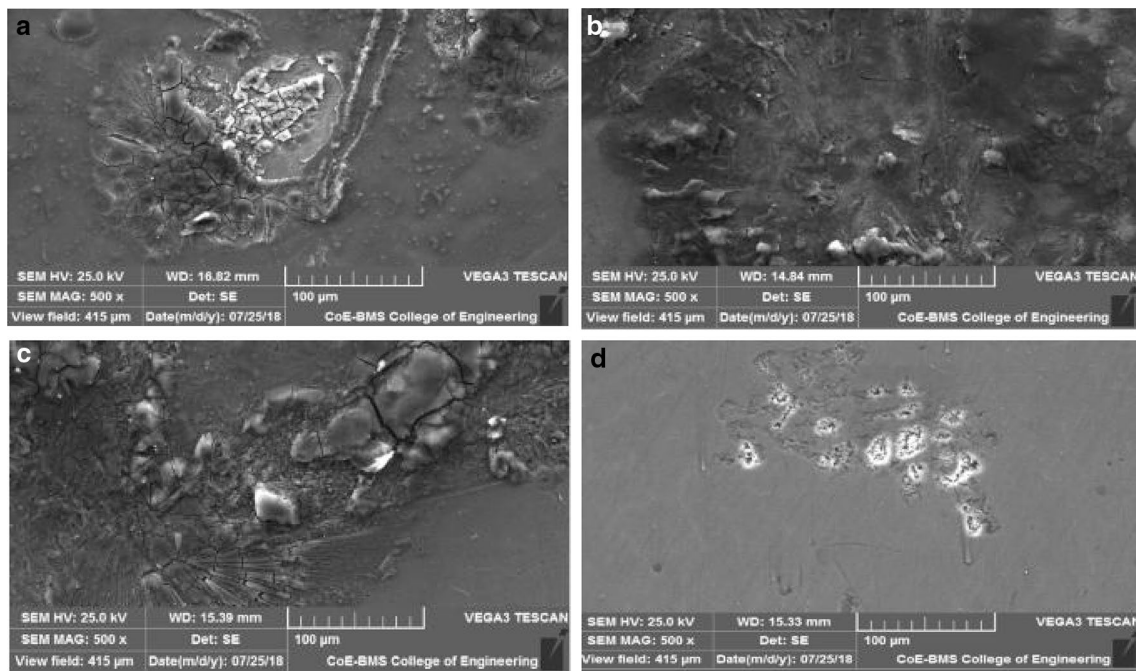


**Fig. 3** SEM micrographs of polarized samples of Al 6065 base metal alloy, 2%, 4% and hybrid composites in 0.1 M H<sub>2</sub>SO<sub>4</sub> medium

composites. Elemental composition of Al 6065 matrix and composites contains intermetallic precipitates like MnO<sub>4</sub> and AlCu<sub>3</sub> which increase the rate of corrosion in composites. SEM micrographs of as casted corroded samples of base metal alloy and its composites after

electrochemical analysis in different electrolytes like 0.1 M HCl, 0.1 M H<sub>2</sub>SO<sub>4</sub> and in 3.5% NaCl are shown in the Fig. 2, 3 and 4.

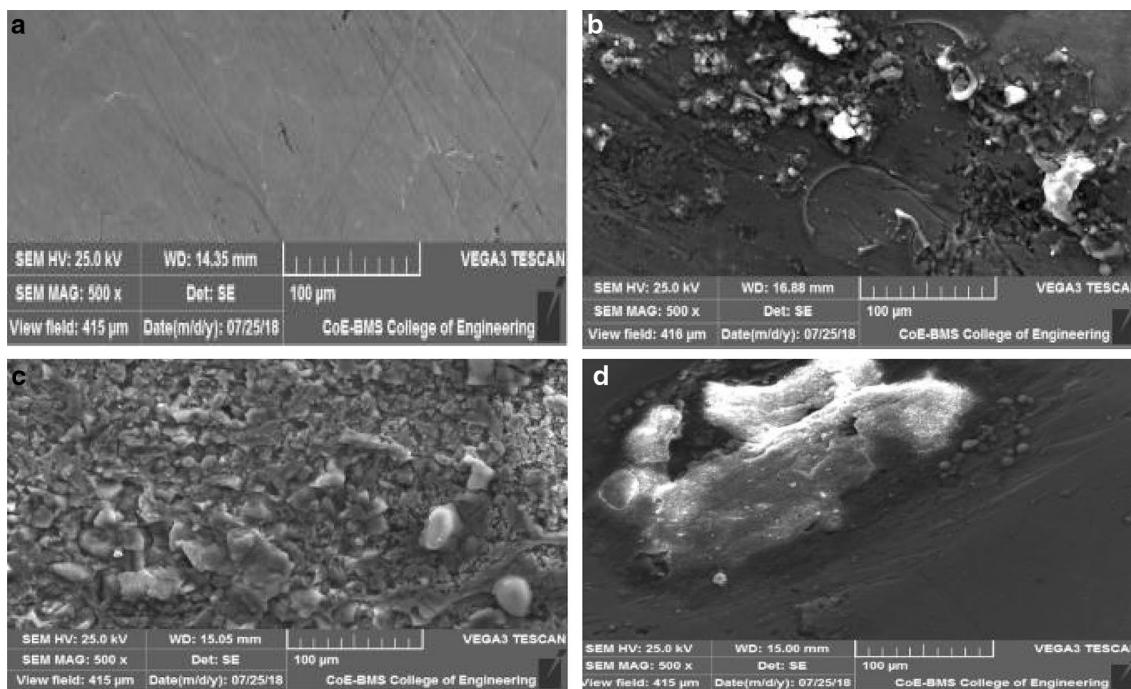


Fig. 4 SEM micrographs of polarized samples of Al 6065 base metal alloy, 2%, 4% and hybrid composites in 3.5% NaCl medium

Table 2 OCP of Al 6065 base metal alloy and its composites in various mediums

SiC Content	OCP (V) in different mediums		
	3.5% NaCl	0.1 M HCl	0.1 M H <sub>2</sub> SO <sub>4</sub>
0%	-0.5508	-0.6721	-0.6007
2%	-0.5608	-0.7068	-0.6286
4%	-0.5682	-0.7114	-0.6437
Hybrid	-0.5502	-0.6695	-0.5897

### 3.2 Electrochemical testing analysis

#### 3.2.1 OCP measurements

OCP were recorded for Al 6065 composites and its base metal alloy in three different electrolyte solutions of 0.1 M HCl, 0.1 M H<sub>2</sub>SO<sub>4</sub> and in 3.5% NaCl. Measured open circuit potentials are given in Table 2. The addition of SiC to the base metal alloy may have result in OCP to more positive, more negative depending on the alloy system, presence and absence of O<sub>2</sub> [13]. From the OCP values it is evident that with increase in % of SiC content in the composites potential shifts towards more negative values and corrosion rates increases, possibility of galvanic corrosion between SiC ceramic particles and Al 6065 matrix [14–18].

#### 3.2.2 Tafel polarization curves

The logarithm of the current density as a function of potential has been taken to generate the polarization curves. In tafel extrapolation near the E<sub>corr</sub> a linear region on both the anodic and cathodic legs has been observed. The slopes of the linear regions are taken as tafel constants named as β<sub>a</sub> and β<sub>c</sub>. E<sub>corr</sub> is obtained by extrapolating these linear regions till they intersect [19]. Log I<sub>corr</sub> values at the point of intersection of co-ordinates will give corrosion current density. Figure 5 are superimposed polarization curves of as casted Al 6065 base metal alloy and its composites in HCl, H<sub>2</sub>SO<sub>4</sub> and in NaCl mediums. Whereas Fig. 6 shows tafel polarization curves of as casted specimens of Al 6065 alloy, 2%, 4% and hybrid composites in different mediums. From the tafel curves it is evident that hybrid composite have lower corrosion rate than compared with base metal alloy. As hybrid composite is casted having equal amounts of SiC and graphite, having low percentage of graphite in the hybrid metal matrix makes the composite better resistant to corrosion [20, 21]. Polarization curve of the hybrid composite shows lowest cathodic, anodic and I<sub>corr</sub> currents and hence it is resistant to corrosion.

#### 3.2.3 EIS measurements

Impedance spectrum shows large capacitive loop at high frequencies and an inductive loop at low frequencies [22].

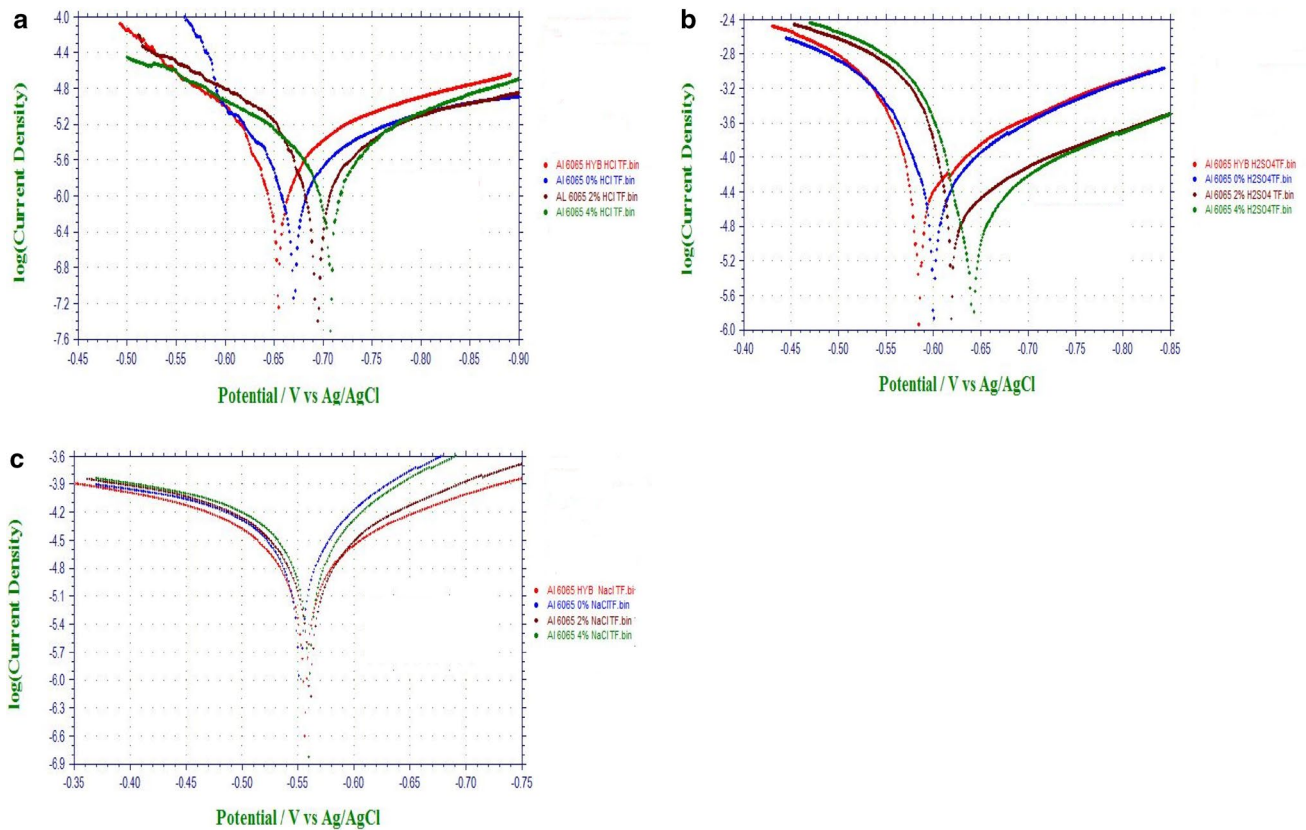


**Fig. 5** Anodic-cathodic polarization curves of Al 6065 base metal alloy, 2%, 4% and hybrid composite in 0.1 M HCl, 0.1 M H<sub>2</sub>SO<sub>4</sub> and 3.5% NaCl mediums

High frequency capacitive semicircle is associated with constant phase element (CPE) and while inductive loop is related with the roughness, inhomogeneities of the solid surface [23]. Diameter of the semicircle is large for hybrid composite in all the mediums [24, 25]. This increase in diameter of the semicircle for hybrid composite affirms that it is higher corrosion resistant [26]. Figure 7 shows complex plane plots obtained for Al 6065 and its composites in 0.1 M HCl, 0.1 M H<sub>2</sub>SO<sub>4</sub>, and 3.5% NaCl solutions.

### 3.2.4 Determination of corrosion rate (CR) using the equation

$$\text{CR (mpy)} = \frac{0.128 \times \text{Equivalent Weight} \times I_{\text{Corr}}}{D} \quad (1)$$

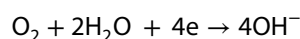
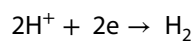
where mpy is mils penetration per year,  $I_{\text{Corr}}$  is corrosion current density ( $\mu\text{A cm}^{-2}$ ) & 'D' is density of the base metal alloy and its composites ( $\text{g cm}^{-3}$ ). Table 3 Shows corrosion rates for Al 6065 base metal alloy and its composites in different mediums, calculated using the above Eq. (1) [27].  $\beta_a$ ,  $\beta_c$  represents anodic tafel slope and cathodic tafel slope whereas  $R_p$  represents linear polarization resistance (LPR).  $R_p$ ,  $\beta_a$ ,  $\beta_c$ ,  $I_{\text{Corr}}$  and corrosion rates which are tabulated in

the Table 3 are obtained from the tafel extrapolation curve which is shown in Fig. 8. Corrosion order of the corrodents are  $\text{NaCl} < \text{H}_2\text{SO}_4 < \text{HCl}$ . Figure 9 shows  $R_p$  is more for hybrid composite in all the mediums which affirms the low corrosion rate of the specimen. It has been observed that corrosion current and corrosion rate increased with increase in percentage of SiC composition in Al 6065 matrix and whereas it is decreased in hybrid composite.

## 4 Discussion

### 4.1 Effect of NaCl medium on the corrosion

From Fig. 16 for 4% Al 6065 composite current decreases in the cathodic side and the cathodic reaction is hydrogen liberation and O<sub>2</sub> reduction.



After reaching  $I_{\text{Corr}}$  and  $E_{\text{Corr}}$  current in the anodic side increases due to aggressiveness of chloride ions.

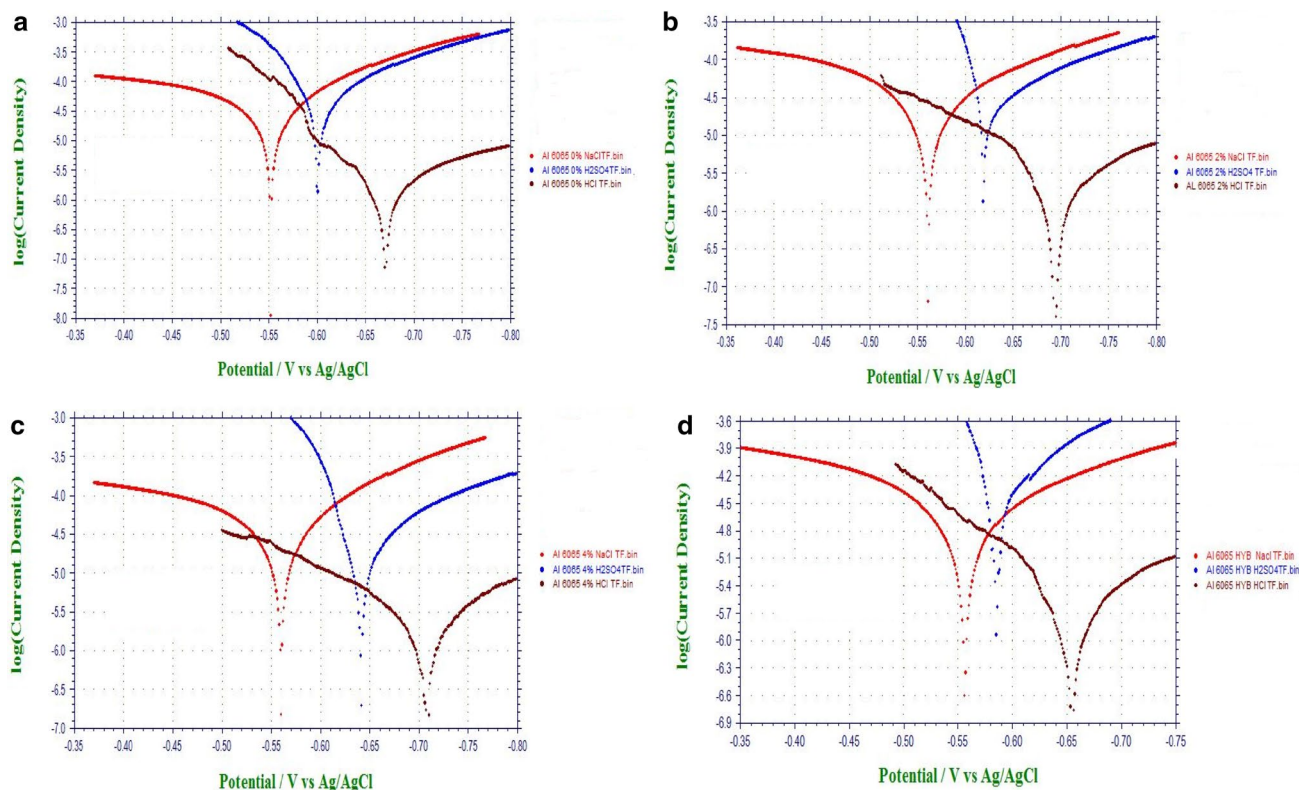
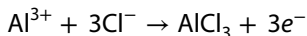
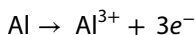
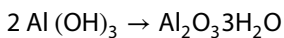
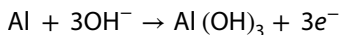


**Fig. 6** Tafel polarization curves of Al 6065 base metal alloy, 2%, 4% and Hybrid composites in different mediums



In the case of 2% composite anodic current decreases and  $E_{\text{corr}}$  shifted to more negative value. For 0% alloy  $E_{\text{corr}}$  shifted to more negative direction with the formation of  $\text{Al}_2\text{O}_3$  layer.



Hybrid composite shows lowest  $I_{\text{corr}}$  due to formation of oxide film and presence of low percentage of graphite particles being anodic to the matrix [8, 28, 29].

### 4.2 Effect of HCl medium on the corrosion

Using HCl as corroding medium, it is attributed that  $\text{Cl}^-$  ions are likely to percolate through the  $\text{Al}_2\text{O}_3$  oxide film there by retarding the self-healing ability of the oxide layer on the metal surface. This results in the formation of intermediate soluble complex.

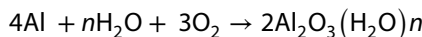


This complex is the cause for the dissolution of the Aluminum ions from the lattice into the solution and leads to thinning of the passive layer on the metal surface and ultimately increasing the corrosion rate in the composites [30–32].

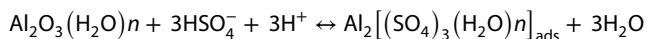
### 4.3 Effect of $\text{H}_2\text{SO}_4$ medium on the corrosion

SiC being cathodic to Al 6065 matrix, corrosion rate increases with increase in percentage of SiC due to breakdown of oxide film on the surface.  $\text{Al}_2\text{O}_3$  layer becomes thin due to  $\text{SO}_4^{2-}$  ions and composites loses its passivation.

Protective Oxide layer formed on the surface of Al 6065 can be destroyed by the action of 0.1 M  $\text{H}_2\text{SO}_4$ .



By the interaction of  $\text{HSO}_4^-$  anions with hydrated film of oxide,  $\text{Al}_2[(\text{SO}_4)_3(\text{H}_2\text{O})_n]$  is formed.



As the complex formed is soluble in aqueous medium, it can be desorbed from the surface leaving free active sites for the attack of anions like  $\text{HSO}_4^-$  or  $\text{SO}_4^{2-}$  [33, 34].

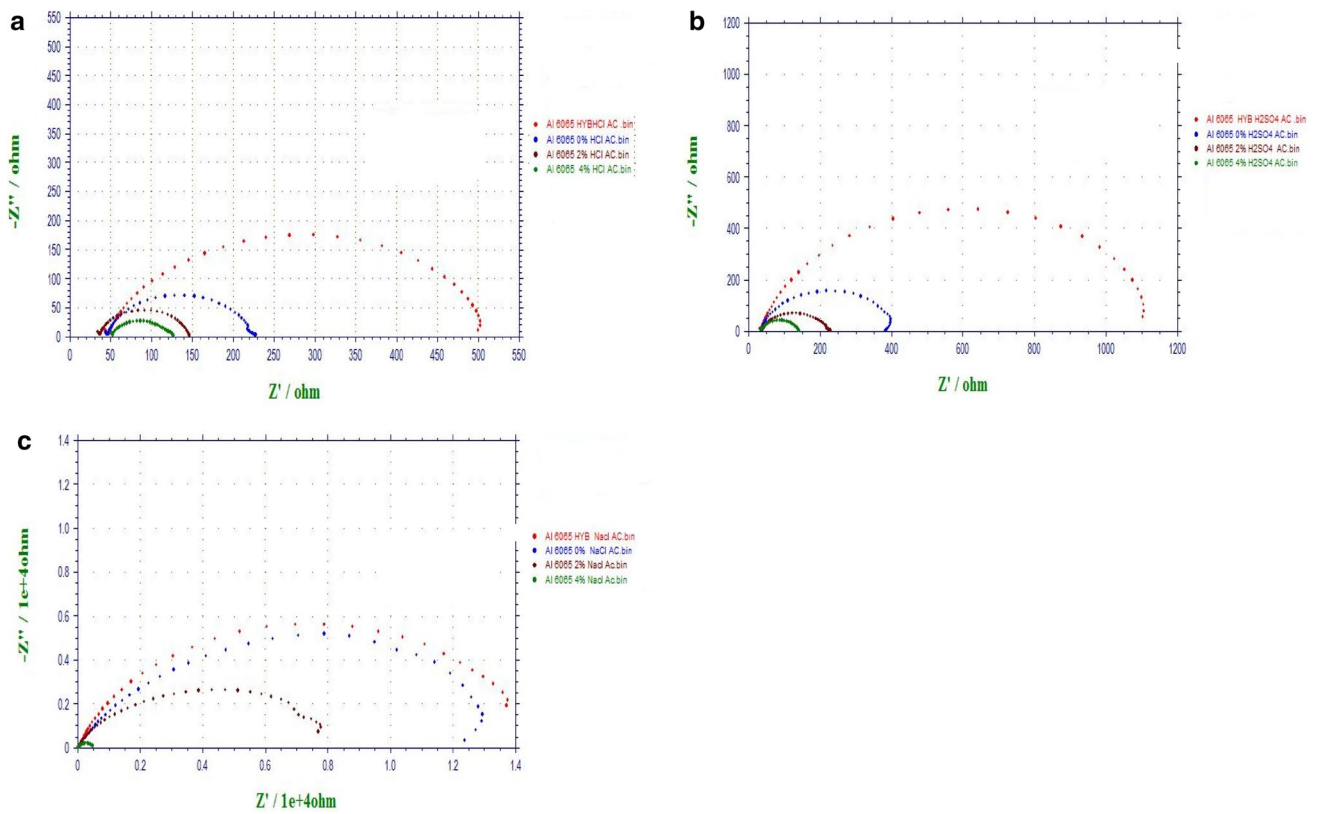


**Fig. 7** Complex plane plots of Al 6065 alloy and its composites 2%, 4% and hybrid composites in 0.1 M HCl, 0.1 M H<sub>2</sub>SO<sub>4</sub> and 3.5% NaCl mediums

**Table 3** Corrosion rates,  $I_{corr}$ ,  $R_p$ ,  $\beta_a$  and  $\beta_c$  of Al 6065 base metal alloy and its composites in different mediums

Medium	% of SiC	$R_p$ (Ohm)	$I_{corr}$ (A cm <sup>-2</sup> ) × 10 <sup>-6</sup>	$\beta_a$ (V)	$\beta_c$ (V)	CR (mpy) × 10 <sup>-5</sup>
0.1 M HCl	0%	324	98.1	7.039	5.315	4.0107
	2%	313	103.9	7.600	6.331	4.2592
	4%	257	150.4	8.247	6.070	6.1832
	Hybrid	864	36.4	5.935	5.586	1.4977
0.1 M H <sub>2</sub> SO <sub>4</sub>	0%	888	44.85	3.644	5.163	1.8454
	2%	886	47.32	4.125	6.752	1.9345
	4%	859	48.72	4.314	6.896	1.9972
	Hybrid	1445	31.75	3.476	6.795	1.3053
3.5% NaCl	0%	11,666	3.787	5.824	3.649	0.1556
	2%	10,568	3.808	5.840	4.158	0.1566
	4%	10,104	3.992	7.714	3.632	0.1632
	Hybrid	12,569	3.728	5.034	4.982	0.1528

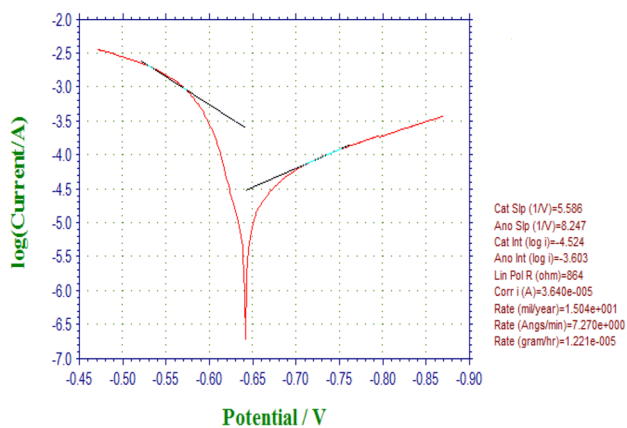


**Fig. 8** Tafel extrapolation curve of Al 6065 hybrid composite using 0.1 M HCl medium

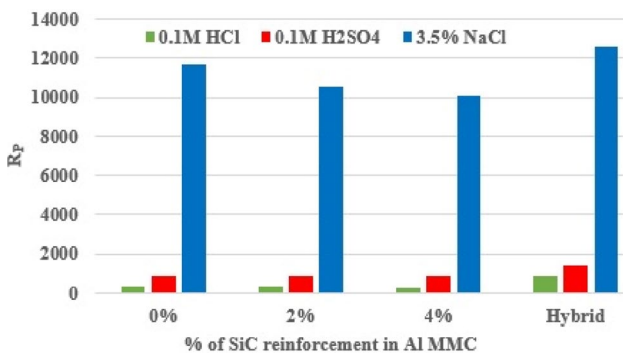


**Fig. 9**  $R_p$  versus % of SiC reinforcement in the Al 6065 metal matrix using 0.1 M HCl, 0.1 M  $H_2SO_4$  and 3.5% NaCl mediums

## 5 Conclusions

The effect of adding 2%, 4% SiC to the base metal alloy and hybrid composite with equal amount of SiC and graphite was investigated by polarization and EIS technique in different inorganic acids and neutral chloride media lead to the following conclusions:-

- Potentiodynamic polarization and impedance studies of the corrosion behavior of 6065 Al alloy and its composites showed that the corrosion resistance of the base metal alloy is greater than that of the composites [35].
- Corrosion rate of hybrid composite exhibited better corrosion resistance compared to the base metal alloy.
- Tafel curves shows  $I_{corr}$  and corrosion rate increased with increase in SiC content in the composites.
- Impedance spectra shows hybrid composite and base metal alloy exhibit better resistance towards corrosion as

the diameter of the semicircle is large for hybrid followed by the base metal alloy.

**Acknowledgements** Authors express our sincere thanks to Vision Group on Science & Technology [VGST] Government of Karnataka with grant number GRD114 for funding the research work, R&D center, Department of Chemistry, Ghousia College of Engineering, Ramanagaram.

## Compliance with ethical standards

**Conflict of interest** The authors declare no conflict of interest.

## References

1. Surappa MK (2003) Aluminum matrix composites: challenges and opportunities. *Sadhana* 28:319–334
2. Lee JC, Ahn JP, Shim JH, Shi ZL (1999) Control of the interface in SiC/Al composites. *Scr Mater* 41:895–900
3. Shi Z, Yang JM, Fan T, Zhang D, Wu R (2000) The melt structural characteristics concerning the interfacial reaction in SiC(p)/Al composites. *Appl Phys A Mater Sci Process* 71:203–209. <https://doi.org/10.1007/s003390000493>
4. Thakur SK, Dhindaw BK (2001) The influence of interfacial characteristics between SiCp and Mg/Al metal matrix on wear, coefficient of friction and micro hardness. *Wear* 247:191–201
5. Wang RM, Surappa MK, Tao CH, Li CZ, Yan MG (1998) Microstructure and interface structure studies of SiCp-reinforced Al (6061) metal-matrix composites. *Mater Sci and Eng A* 254:219–226
6. Winkler S, Flower H (2004) Stress corrosion cracking of cast 7XXX aluminum fiber reinforced composites. *Corros Sci* 46:903
7. Bobic B, Mitrovic S, Babic M, Bobic I (2009) Corrosion of aluminum and zinc-aluminum alloys based metal-matrix composites. *Tribol Ind* 31:44–52
8. Sherif E-SM, Almajid AA, Lateif FH, Junaedi H (2011) Effects of graphite on the corrosion behavior of aluminum-graphite composite in sodium chloride solutions. *Int J Electrochem Sci* 6:1085–1099
9. Lateif FH, Sherif E-SM, Almajid AA, Junaedi H (2011) Corrosion behavior in 3.5% NaCl solutions of  $\gamma$ -TiAl processed by electron beam melting process. *J Anal Appl Pyrolysis* 92:485–492
10. Winston Revie R (2011) Uhlig's corrosion hand book. Wiley, London
11. Seah KHW, Girish BM, Satish BM (1998) Effect of artificial ageing on Tensile strength of ZA-27 short glass fiber reinforced Composite. *J Inst Eng* 38:21–26
12. Abbass MK, Hassan KS, Alwan AS (2015) Study of corrosion resistance of Aluminum alloy 6061/SiC composites in 3.5% NaCl solution. *Int J Mater Mech Manuf* 3:31–35
13. Trzaskoma PP, McCafferty E (1983) Corrosion behavior of SiC/Al metal matrix composites. *J Electrochem Soc Electrochem Sci Technol* 130:1804–1809
14. Dabrzanski LA, Wladarczyk A, Adamiak M (2005) Structure properties and corrosion resistance of PM composite material based on ENAW-2124 aluminum alloys reinforced with  $Al_2O_3$  ceramic particles. *J Mater Proc Technol* 162(163):27–31
15. Gurrappa I, Prasad VVB (2006) Cold spraying SiC/Al metal matrix composites: effects of SiC contents and heat treatment on microstructure, thermophysical and flexural properties. *Mater Sci Technol* 22:115



16. Kamaj JA (2015) Comparison of potentiodynamic polarization and weight loss measurements techniques in the study of corrosion behavior of 6061 Al/SiC composite in 3.5 M NaCl solution. *Asian J Appl Sci* 3:264–270
17. Dikici B, Tekmen C (2015) A comparative study: the combined effect of the cold working and age hardening processes on pitting behavior of Al/SiC metal matrix composites under saline environment. *J Compos Mater* 50(4):471–480. <https://doi.org/10.1177/0021998315576554>
18. Galvele JR (2005) Tafel's law in pitting corrosion and crevice corrosion susceptibility. *Corros Sci* 47:3053–3067. <https://doi.org/10.1016/j.corsci.2005.05.043>
19. King JD (1989) Characterization of the corrosion of a P-130X graphite fiber reinforced 6063 aluminum metal matrix Composite. Dissertation, Naval Postgraduate School
20. Seah KHW, Sharmas FSC, Girishs BM (1997) Corrosion characteristics of ZA-274 graphite particulate composites. *Corros Sci* 39:1–7
21. Afifi MA (2014) Corrosion behavior of zinc-graphite metal matrix composite in 1 M of HCl. *Corrosion* 45:50. <https://doi.org/10.1155/2014/279856>
22. Reena Kumar PD, Nayak J, Shetty AN (2016) Corrosion behavior of 6061/Al-15 Vol. Pct. SiC (p) composite and the base alloy in sodium hydroxide solution. *Arab J Chem*. <https://doi.org/10.1016/j.arabjc.2011.12.003>
23. Ehsani A, Mahjani MG, Moshrefi R, Mostanzadeh H, Shayeh JS (2014) *RSC Advances* 4:20031–20037. <https://doi.org/10.1039/c4ra01029a>
24. Yu-Mei Han, X.Grant Chen (2015) Electrochemical behavior of Al-B<sub>4</sub>C metal matrix composites in NaCl solution. *Materials*. doi: 103390/ma8095314
25. Sherif ESM, Abdo HS, Khalil KA, Nabawy AM (2016) Effect of titanium carbide content on the corrosion behavior of Al-TiC composites processed by high energy ball mill. *J Electrochem Sci Int*. <https://doi.org/10.20964/2016.06.18>
26. Rebeiro DV, Souza CAC, Abrantes JCC (2015) Use of electrochemical impedance spectroscopy (EIS) to monitoring the corrosion of reinforced concrete. *Ibracon*. <https://doi.org/10.1590/S198341952015000400007>
27. Achutha Kini U, Prakasha Shetty S, Divakara Shetty M, Isloor A (2011) Corrosion inhibition of Al6061-SiC<sub>p</sub> composite in 0.5 M hydrochloric acid. *Int Conf Chem Chem Process IPCBEE* 10:127–132
28. Alsamuraee AMA, Ameen HA, Al-Rubaiey SIJ (2011) Evaluation of the pitting corrosion for aluminum alloys 7020 in 3.5% NaCl solution with range of temperature (100–500)°C. *Am J Sci Ind Res* 2:283–296. <https://doi.org/10.5251/ajsir.2011.2.2.283.296>
29. McCafferty E (2003) Sequence of steps in the pitting of aluminum by chloride ions. *Corros Sci* 45:1421–1438
30. Shetty KS, Shetty AN (2015) Studies on corrosion behavior of 6061 Al-15 vol. pct. SiC(p) composite in HCl Medium by electrochemical Techniques. *Surf Eng Appl Electrochem* 51:374–381
31. Ambat R, Dwarakadasa ES (1993) Effect of chloride ion concentration during corrosion of medium strength aluminium alloys 8090, 2091 and 2014. *Br Corrs J* 28(2):142
32. Al-Turkustani A, Arab S, Al-Dahiri R (2010) Aloe plant extract as environmentally friendly inhibitor on the corrosion of aluminum in hydrochloric acid in absence and presence of iodide ions. *Mod Appl Sci* 4:105–124
33. Arellanes-Lozada P, Olivares-Xometl O, Guzman-Lucero D, Likhanova NV, Dominguez-Aguilar MA, Lijanova IV, Arce-Estrada E (2014) The inhibition of aluminum corrosion in sulfuric acid by poly (1-vinyl-3-alkyl-imidazolium hexafluorophosphate). *Materials* 7:5711–5734. <https://doi.org/10.3390/ma7085711>
34. Sanni O, Popoola AP (2017) Gluconates as corrosion inhibitor of aluminum in various corrosive media. Aluminum alloys-recent trends in processing, characterization, mechanical behavior and applications. <http://dx.doi.org/10.5772/intechopen.71467>
35. Pinto GM, Jagannath Nayak A, Shetty N (2009) Corrosion behavior of 6061 Al-15 Vol. Pct. SiC composite and its base alloy in a mixture of 1:1 hydrochloric and sulphuric acid medium. *Int J Electrochem Sci* 4:1452–1468

**Publisher's Note** Springer Nature remains neutral with regard to jurisdictional claims in published maps and institutional affiliations.